Article

An Energy Analysis of a Slab Preheating Chamber for a Reheating Furnace

Kitipong Kangvanskol and Chittin Tangthieng*

Department of Mechanical Engineering, Faculty of Engineering, Chulalongkorn University, Phayathai Rd., Wangmai, Patumwan, Bangkok 10330, THAILAND
*E-mail: QED690@yahoo.com (Corresponding author)

Abstract. The iron and steel industry is one of the major industries for developing countries, and it is ranked as one of the industrial sectors that have the highest energy consumption. It is also served as a primary industry that provides materials to secondary industries as well. This present study focuses on a slab, a product from a steelmaking process, which will be sent to a hot-rolling mill to form a final product. Before the rolling process, slab is heated to a proper temperature by charging into a reheating furnace. Heat is generated by a combustion process from direct-fired burners. In general, heat loss from the reheating furnace occurs by several mechanisms including the flue gas loss. Although a recuperator is used to reduce heat loss by recovering some of that to preheat the combustion air, the exit flue gas temperature is still as high as 350-450°C. This research paper aims for the investigation of the energy efficiency resulted from the implementation of a slab preheating chamber before charging into a reheating furnace. Four different sizes of the preheating chamber are selected as the case studies for the energy analysis. Another consideration includes the acid dew point of the flue gas as the lowest criteria for the flue gas temperature. The result indicates that the flue gas temperatures are above the acid dew point for all four cases under consideration. The slab temperatures increase from the ambient temperature of 30°C to 59.52°C, 75.98°C, 84.98°C and 89.46°C, respectively, before begin charged into the reheating furnace. As a result, the fuel energy consumption after the implementation of the reheating chamber is reduced by 0.94%, 1.46%, 1.75% and 1.89%, respectively comparing to the furnace without the reheating chamber. The reheating furnace efficiency also increases from 69.88% to 70.54%, 70.92%, 71.13% and 71.22%, respectively.

Keywords: Reheating furnace, preheating chamber, flue gas.

1. Introduction

Iron and steel industry is one of the major industries for developing countries because it is a primary industry that provides raw materials for a secondary one such as automotive, food, electronic industries. It can be divided into 3 sections, an upstream section industry which produces a raw steel product, a middle stream section which produces a semi-finished steel product and a downstream section which produces a finish steel product that we will focus on. This present study focuses on a slab, a product from a steelmaking process, which will be sent to a hot-rolling mill to form a final product. Before the rolling process, a slab must be heated to a proper temperature of 1100-1250°C in a reheating furnace. Heat is generated by direct combustion from fuel resulting in the flue gas as a product of combustion. A reheating furnace is divided into 3 zones: preheating, heating, and soaking zones. The preheating zone is a place where hot flue gas transfers heat to the slab by a counter flow manner. The heating zone is used to continuously heat the slab to a desired temperature whereas the soaking zone is used to supply enough heat to make slab temperature uniform. The flue gas after the combustion process can reach temperature up to 800°C, which still contains a large amount of thermal energy. A favorite method of utilizing this waste heat from the flue gas is by using a recuperator to preheat the combustion air to 300-400°C. With a very high efficient device such as recuperative burners, it can raise the combustion air temperature up to 1000°C [1, 2].

From the studies of Jiang et al. [3] and Chen et al. [4], it is found that the flue gas temperature after leaving a recuperator is still at approximately 350-450°C. Therefore, the idea is to utilize the remaining energy in the flue gas to heat slabs before charging them into a reheating furnace in order to save more energy. A study of Minxing et al. [5] shows that from the numerical prediction, Biot number of a billet is 0.03 which is less than 0.1. Therefore, the lumped capacitance method is valid to calculate temperature profile of the billet. From his calculation by 1.48 hours, the temperature of the billet rises from 3.5°C to 315°C with flue gas temperature of 815°C, and this preheat method can save energy by 278.12 kJ/kg. This can be converted to the cost saving of $215,086 per year with a capital cost of $1,250,000 and 3 years of the payback period. From a study of Shamanian and Najafizadeh [6] on hot and warm charging process, it is found that every 100°C increase of preheat temperature of steel before loading in to a furnace can save 80-120 kJ/kg of energy. It is reported from a study of Ross [7] that 20 percent of hot charge slabs at 600°C leads to the energy reduction by 7 percent. A batch-type preheating device is also found useful for a glass furnace [8]. The charged material can be heated up to 350°C depending on the condition of the flue gas.

This present study focuses on the energy saving from the preheated slab by the flue gas. The objective is to determine the mass and heat balance of the reheating furnace by the field data to determine the slab and flue gas temperatures. A heat balance model of the preheating chamber with is developed. The energy efficiency after the implementation is investigated for four different cases based on the sizes of the chamber.

2. Reheating Furnace

In this present study the reheating furnace has a capacity of 275 tonne/hr and uses fuel oil for combustion. The furnace is a walking heart type furnace with the preheating, heating and soaking zones as shown in Fig. 1. A number of burners in each of these three zones are eighteen, eighteen, and forty five, respectively. The inner size of the furnace is 12,650x42,000 mm. This furnace operates 24 hours a day. The average dimension of the charged slab is 250x1260x9240 mm with the weight of 22.88 tonne per each slab.
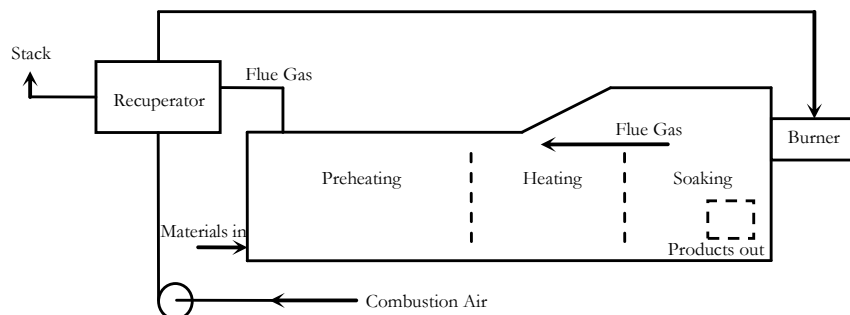
Fig. 1.   A Schematic Diagram of a Reheating furnace.

The heat source for a reheating furnace originates from combustion of the fuel. A complete combustion takes place when there is the proper ratio between oxygen and fuel, namely a stoichiometric combustion, is provided. For fuel oil, the composition and its properties are listed in Tables 1 and 2 [9]. On the other hand, the oxidizer for combustion process is air which is composed of 79 percent of nitrogen and 21 percent of oxygen.

Table 1.   Composition of fuel oil.

Element	Percent by weight
C	86.4
H	11.6
S	2.0

Table 2.   Properties of fuel oil.

Properties		Dimension
Molecular weight	5.32	kg/kmol
Specific gravity	0.964	-
Specific heat	1.884	kJ/kg-K
Heating value	43069.63	kJ/kg

The reaction between the fuel oil and air as reactants and flue gas as products of combustion can be written as shown in Eq. (1).

$$
\begin{aligned}
&C_{0.3836}H_{0.6131}S_{0.0033} + n_{stoic}\lambda\left[O_2 + 3.76N_2\right] \\
&\rightarrow 0.3836CO_2 + 0.0033SO_2 + 0.3065H_2O \\
&+ n_{stoic}\left[\lambda\text{-}1\right]O_2 + n_{stoic}\lambda\left[3.76N_2\right]
\end{aligned}
\tag{1}
$$
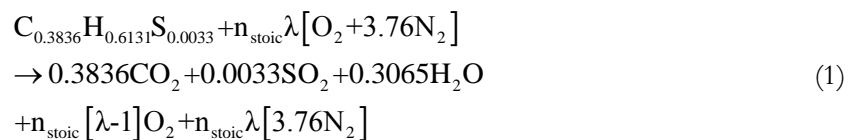
In practice, the stoichiometric combustion cannot be achieved due to the limitation of the air-fuel mixing and combustion time [10]. Therefore, additional air must be provided to guarantee that the unburned fuel no longer remains in the combustion process. A variable representing the amount of this extra air during the combustion process is called λ, which is defined as the actual air-fuel ratio to the stoichometric one as shown in Eq. (2).

$$
\lambda = \frac{AF_{actual}}{AF_{stoic}} == \frac{n_{actual}}{n_{stoic}}
\tag{2}
$$

From Eq. (1), if λ is set to unity, it means that combustion process takes place at the stoichiometric condition. As a result, the value of n_{stoic} can be determined by the chemical equation balance based on the fuel composition. In case of fuel oil, the value of n_{stoic} is equal to 0.5402 kmol$_{O2}$/kmol$_{fuel}$. On the other hand, if λ is greater than unity, the combustion process takes place with excess air. In practice, λ can be determined by measuring the percent of oxygen in the flue gas by an oxygen sensor. The relation between the mole fraction of oxygen on wet basis and the value of λ can be expressed in Eqs (3) and (4) as follow:

$$
\frac{\%O_2}{100} = \frac{(\lambda\text{-}1)n_{stoic}}{0.6934 + (\lambda\text{-}1)n_{stoic} + 3.76\lambda n_{stoic}}
\tag{3}
$$

$$
\lambda = \frac{0.5402 + 0.153\left(\dfrac{\%O_2}{100}\right)}{0.5402 - 2.571\left(\dfrac{\%O_2}{100}\right)}
\tag{4}
$$

3. Mass and Heat Balance of The Furnace

In this study, the mass and heat balance of the reheating furnace can be performed based on the data obtained by the field measurement.

3.1. Mass Balance

The fuel mass flow rate is obtained by the direct measurement of the fuel flow meter. The volume flow rate of the combustion air is measured directly from the orifice plate and the pressure transmitter. The unit of the volume flow rate provided by the measuring device is Nm^3/hr. Thus, the air density at the normal condition of 1.293 kg/m^3 is used to convert the volume flow rate to the mass flow rate. The output mass flow rate of flue gas is the consequence of the mass balance by combining the fuel mass flow rate with the air one under the assumption of no leak between the furnace and its surrounding.

Table 3.   Mass flow rate of a reheating furnace.

Input	kg/s	Output	kg/s
1. fuel mass flow rate	1.82	1. flue gas mass flow rate	26.31
2. air mass flow rate	24.49		
Total	26.31	Total	26.31

3.2. Heat Balance of the Reheating Furnace and the Recuperator

Since the furnace and the recuperator is operated under the steady state condition, the heat balance of both can be combined and presented in a Sankey diagram [11, 12] as shown in Fig. 2.
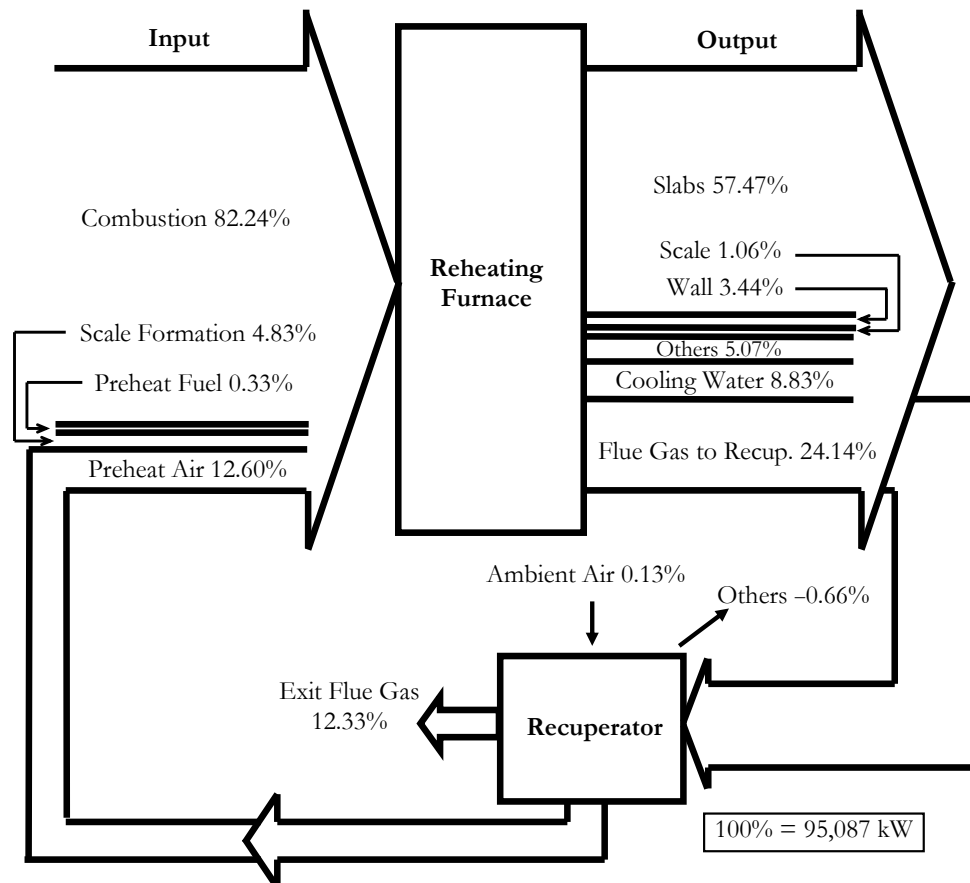
Fig. 2.   Heat balance diagram of the reheating furnace and the recuperator.

4. Calculation Methodology

The operation of the preheating chamber related to the reheating furnace is depicted in Fig. 3. This preheating chamber is a batch-type one, which can be used in many types of industrial furnaces [13].
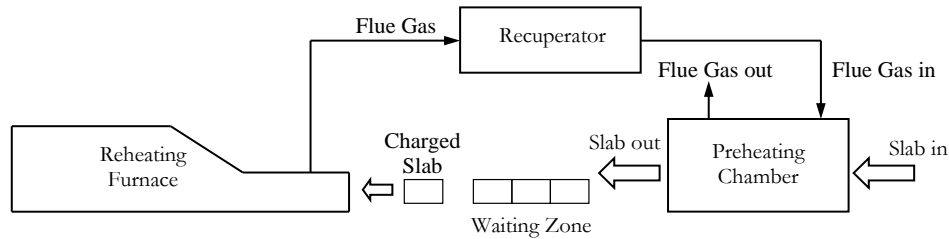
Fig. 3.   Operation of the preheating chamber related to the reheating furnace.

The number of slabs fed into the preheating chamber will relate to the plant production rate of 200.2 tonne/hr, which is equivalent to the production rate of 9 pieces of slab per hour. For example, if the maximum capacity of the preheating chamber per one batch is 9 pieces, the batch time will be less than an hour due to additional transportation time between the furnace and the chamber itself. This transportation time is estimated to be 25 percent of the furnace production time. Thus, in case of 9 pieces of slab in the preheating chamber, the production time will be one hour with the transportation time of 15 minutes and the batch time of 45 minutes. In this study, the capacity per one batch of the preheating chamber is selected to be 9, 18, 27 and 36 pieces with the batch time of 45, 90, 135 and 180 minutes, respectively, and the transportation time will be calculated in the similar manner.

When the preheating process is finished, all slabs must be conveyed out of the preheating chamber and wait until being charged into the furnace. Thus, the temperature of the preheated slabs will decrease due to the heat loss to the environment during the waiting period. Note that each preheated slab has different waiting period such that the preheated slab located nearest to the furnace charge door will have the shortest waiting period.

The design calculation of the batch-type preheating chamber consists of three parts. The first one is the increase of slab temperature during the batching period. The second one is the calculation of the temperature reduction during the waiting period. The last one is the prediction of acid dew point since the existence of sulfur in fuel oil.

4.1.   Slab Temperature During the Batching Period

For the slab-temperature calculation, the slab is placed in the preheating chamber as depicted in Fig. 4. The flue gas is allowed to pass through both sides of the slab surfaces. The calculation is performed by selecting two small control volumes: the upper control volume contains the flue gas flow above the slab surface. The lower control volume contains a half of the slab since the flow of the flue gas is symmetry on both sides of the slab as shown in Fig. 4.
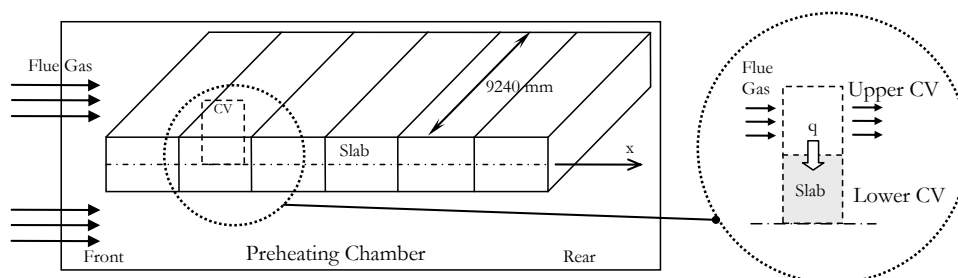
Fig. 4.   Control volumes for the flue gas and the slab.

At the initial time, the heat transfer between the upper control volume and the lower one is calculated at the first slab at the front of the chamber, causing the increase of the slab temperature. Next, the reduction of the flue gas temperature of the upper gas control volume is estimated. The repeated calculation is performed by marching along the x-axis to the last slab at the rear of the chamber. The overall procedure is repeated again to the next time step until the final time is reached. It should be noted that the Biot number of the slab is calculated to be 0.03, which is less than 0.1, leading to the validity of the lumped capacitance approach.

The heat transfer of the flue gas can be calculated by assuming the internal flow through a rectangular slot. The Reynolds number based on the hydraulic diameter of the rectangular slot can be determined.

The value of ρ of the flue gas is approximated by 0.5215 kg/m^3 and μ is approximated by using the viscosity of air at the same temperature. The mean velocity, U, is calculated by the mass flow rate of the flue gas given by Table 3 divided by the slot cross-sectional area of 0.25x10 m^2. The convective heat transfer coefficient and the friction factor of the flue gas are given by Eq. (5) and Eq. (6), respectively [14, 15].

$$Nu_D = \frac{hL}{k} = \frac{(f/8)(\mathrm{Re}_D - 1000)\mathrm{Pr}}{1 + 12.7(f/8)^{1/2}(\mathrm{Pr}^{2/3} - 1)} \tag{5}$$

$$\frac{1}{f^{1/2}} \approx 2.0\log\left(0.64\,\mathrm{Re}_{D_h}\,f^{1/2}\right) - 1.19 \tag{6}$$

4.2. Slab Temperature During the Waiting Period

Because of the validity of the lumped capacitance method, the temperature profile of the slabs due to heat loss to the environment is recommended by Shamanian and Najafizadeh [6] as shown in Eq. (7).

$$T = (T_o - T_{os})e^{\left[-0.0530\left(\frac{1}{B} + \frac{1}{nH}\right)\tau^{0.848}\right]} + T_{os} \tag{7}$$

T_0 and T are initial and final temperatures, respectively. T_{os} is the ambient temperature and τ is the elapse time. H and B is the thickness and width of each slab whereas n is the number of stag levels

4.3. Acid Dew Point

Acid dew point of the flue gas is an important criterion to consider due to the sulfur content in fuel oil. The correlations to related the acid dew point and the composition of the flue gas have been proposed by many researchers [16-18]. From the work of ZareNezhad and Almanian [19], the estimated acid dew point obtained from the Verhoff and Banchero equation [16] has the highest values among the correlations under their interest. The existence of acid in the flue gas originates from the conversion of SO_2, produced by the combustion process, to SO_3. However, the conversion mechanism from SO_2 to SO_3 is rather complicated since it depends on many factors such as flue gas temperature, fuel composition and the amount of excess air [20]. A study of Tan et al. [21] shows that the estimated conversion factor of SO_2 to SO_3 could be as high as 5 percent depending on the fuel. Thus, this study will use the conversion factor of 5 percent to estimate the amount of SO_3 in the flue gas. Thus, the acid dew point of the flue gas can be calculated by the Verhoff and Banchero equation as follows:

$$\frac{1000}{T_{Dew}} = 2.276 - 0.0294\ln(P_{H_2O}) - 0.0.0858\ln(P_{SO_3}) + 0.0062\ln(P_{H_2O})\ln(P_{SO_3}) \tag{8}$$

T_{dew} is the acid dew point temperature in Kelvin and the partial pressures of H_2O and SO_2 are in mmHg.

5. Results and Discussion

The flue gas analysis can be performed by the field data measurement on November 2011. The average flue gas temperature and total pressure after leaving the recuperator is 408.4^{o}C and 101.2 kPa with the average percent of O_2 of 0.988% (wet basis). The mole fractions and the partial pressures of each component of the flue gas calculated from Eqs. (1) to (4) are presented in Table 4.

Table 4.   Mole fractions and partial pressures of the flue gas.

	Mole Fraction (%)	Partial Pressure (mmHg)
CO_2	14.2155	108.0274
SO_2	0.1162	0.8828
H_2O	11.3583	86.3128
O_2	0.9883	7.5105
N_2	73.3156	557.1328
SO_3	0.0061	0.0465

By employing Eq. (8) using the partial pressures in Table 4, the acid dew point is estimated to be 157°C. As a result, the average flue gas temperature after leaving the preheating chamber must be higher than this acid dew point to prevent acid condensation.

The increase of the slab temperature and the reduction of the flue gas temperature during the batching period with different capacities per one batch are depicted in Figs. 5 to 8. Note that the increment dx and the time interval dt using for the calculation is set to be 0.01 m and 1 s, respectively. The batch time of these four cases has been described earlier in section 4.
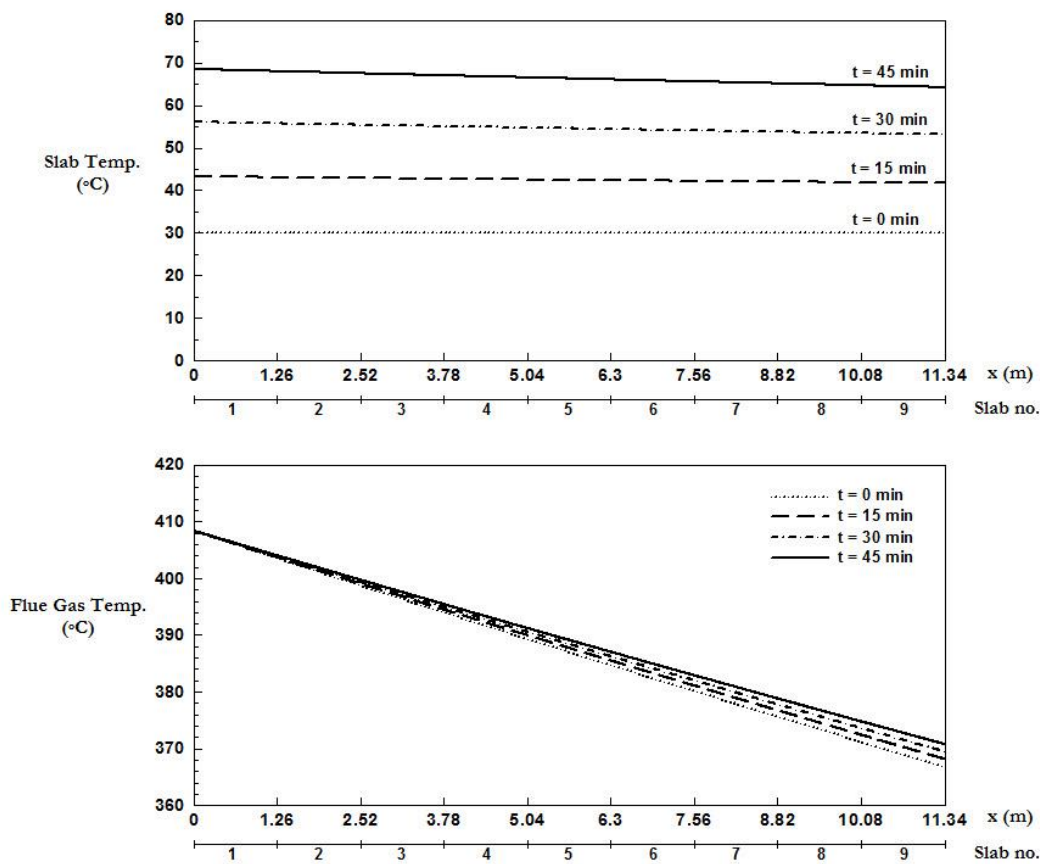
Fig. 5.   The slab and flue gas temperatures with the capacity of 9 pieces of slab per one batch.
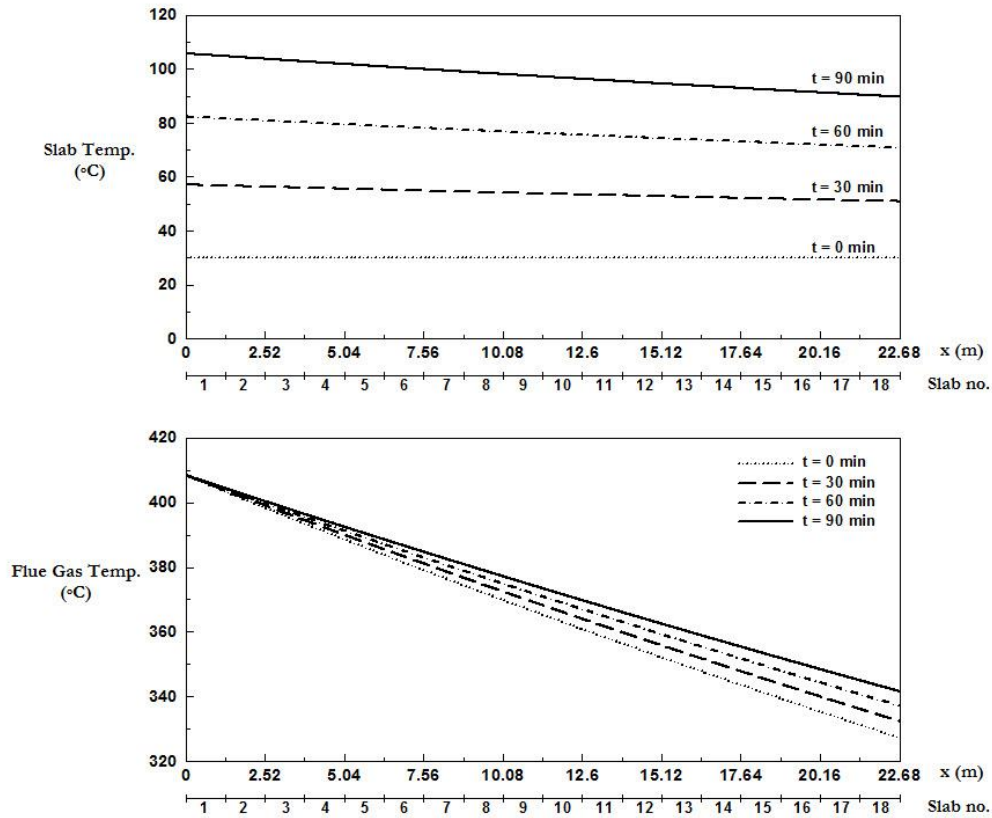
Fig. 6.   The slab and flue gas temperatures with the capacity of 18 pieces of slab per one batch.
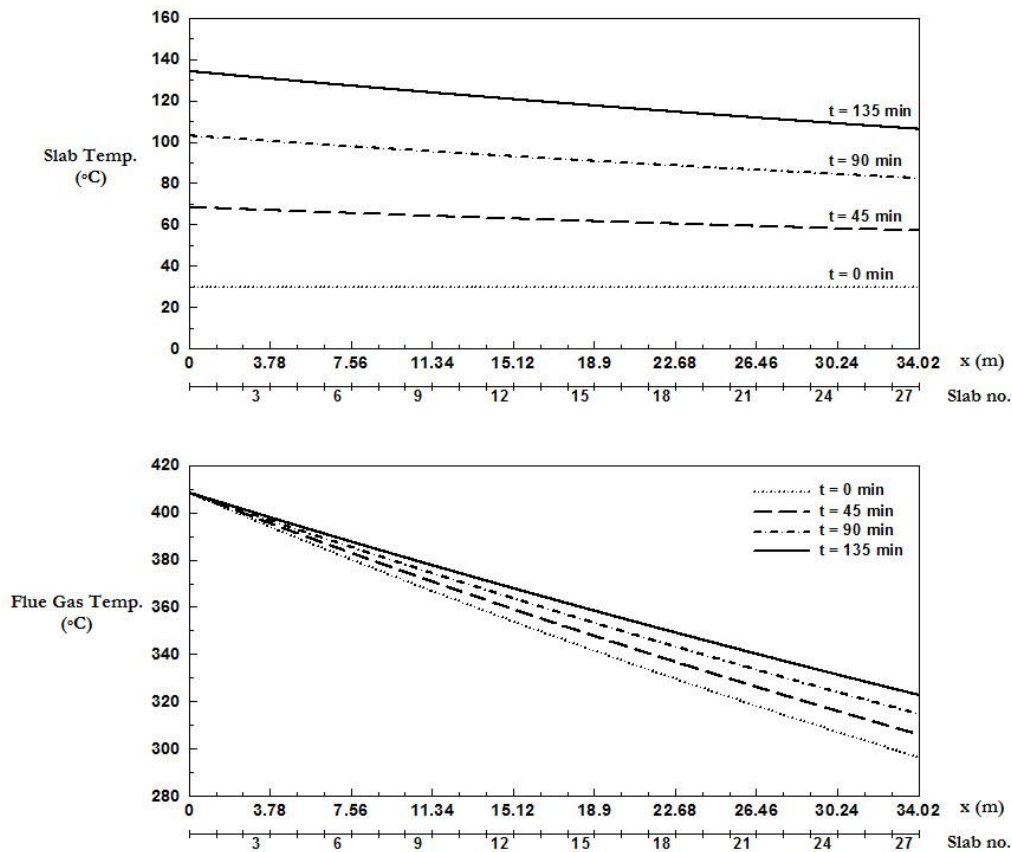
Fig. 7.   The slab and flue gas temperatures with the capacity of 27 pieces of slab per one batch.
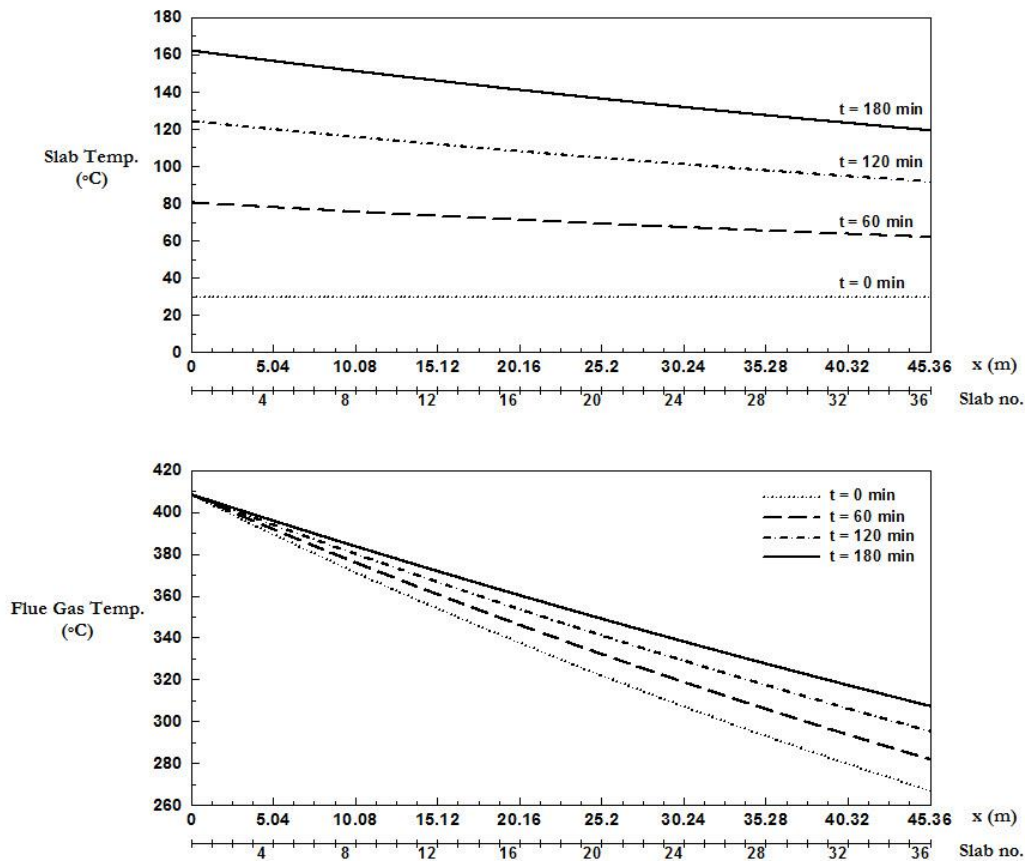
Fig. 8.   The slab and flue gas temperatures with the capacity of 36 pieces of slab per one batch.

At a given time, the slab temperature decreases with increasing value of x whereas the flue gas temperature also decreases with increasing value of x as well. At the flue gas travels along the x-axis, the temperature of the flue gas will drop due to the heat transfer to the slab, causing less temperature difference between the flue gas and the slabs. Therefore, at a higher value of x, the heat transfer rate decreases leading to the reduction of the slab temperature along the x-axis. As time goes by, the slab temperature starts increasing throughout the entire slabs due to the thermal energy storing within the slabs themselves. On the other hand, the flue gas temperature along the x-axis does not drop that much comparing to that at the initial time because heat transfer rate between the slabs and the flue gas decreases with increasing time.

Quantitatively, it is observed from Figs. 5 to 8 that the lowest flue gas temperatures of all four cases are located at the rear of the chamber. The values are estimated to be 366.80°C, 327.37°C, 296.58°C and 267.03°C, respectively. Those values are above the acid dew point of 157°C, leading to the nonexistence of the acid condensation. After the batching process, the average temperatures of all slabs in the chamber for the capacities of 9, 18, 27 and 36 pieces of slab per one batch are 66.33°C, 95.57°C, 119.45°C and 139.19°C, respectively. At the end of the batching period, the slab temperature decrease during the waiting period according to Eq. (7). Consequently, the average temperatures of all slabs in these four cases decrease to 59.52°C, 75.98°C, 84.98°C and 89.46°C, respectively. It can be seen that in case of a chamber with 36 pieces of slab per one batch, although the slab temperature increase to the highest value, that temperature also decrease the most owing to the longest waiting period.

The benefit of the preheating chamber is to raise the slab temperature above the ambient one before being charged into the reheating furnace. The energy saving can be estimated by the amount of thermal energy used to increase the temperature of the slab from the ambient temperature to the preheating one. With a given steel specific heat of 0.78 kJ/kg-K, the thermal energy carried by the slabs in case of the chamber for the capacities of 9, 18, 27 and 36 pieces of slab per one batch is 732.9 kW, 1,141.4 kW, 1,364.9 kW and 1,476.1 kW, respectively. By considering the Sankey diagram in Fig. 2, this amount of energy will be deduced from the input thermal energy from the fuel combustion. As a result, the Sankey diagram for these four cases is given in Fig. 9 and Table 5.
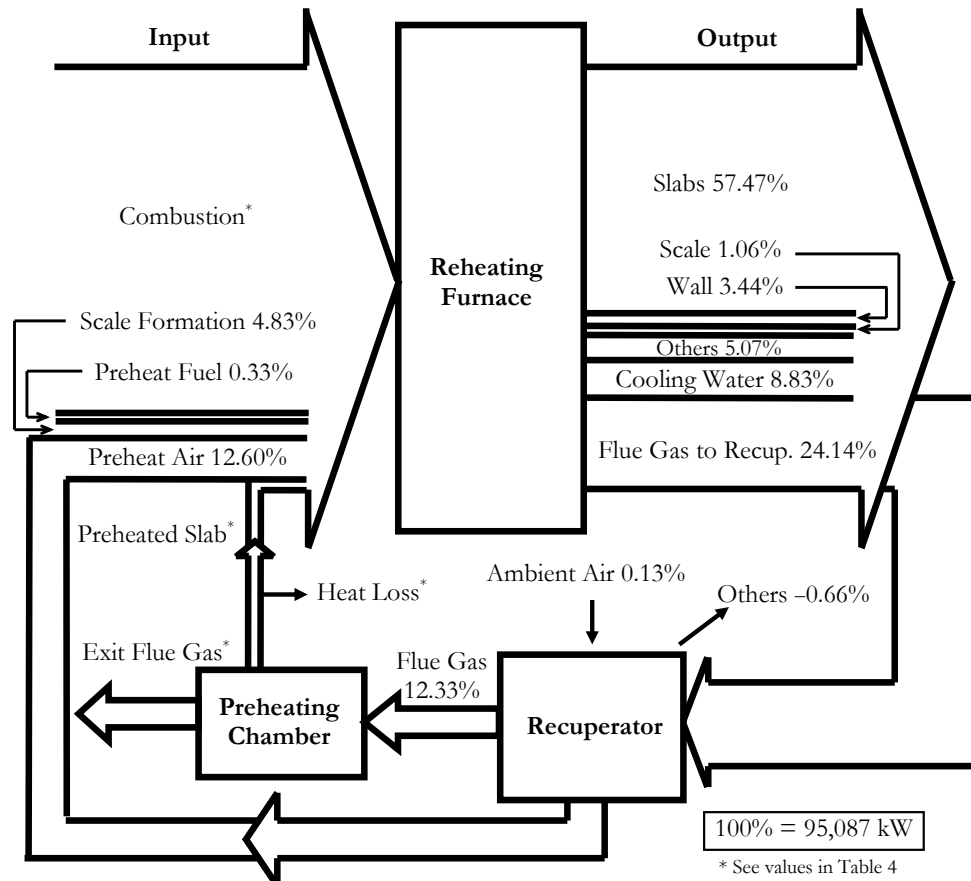
Fig. 9.   The Sankey diagram for four different cases under consideration.

Table 5.   The values corresponding to Fig. 9.

No. of Slab per Batch	Combustion kW (%)	Preheated Slab kW (%)	Heat Loss kW (%)	Exit Flue Gas kW (%)
9	77,471 (81.47)	733 (0.77)	16,892 (0.18)	10,822 (11.38)
18	77,062 (81.04)	1,141 (1.20)	48,642 (0.51)	10,096 (10.62)
27	76,839 (80.81)	1,365 (1.44)	85,562 (0.90)	9,504 (9.99)
36	76,728 (80.69)	1,476 (1.55)	123,446 (1.30)	9,014 (9.48)

By comparing the case before the implementation and the four cases after the implementation shown in Table 5, it can be seen that the amount of the waste energy from the flue gas is reduced from 12.33% down to 11.38%, 10.62%, 9.99% and 9.48%, respectively.   Thus, the amount of the fuel combustion decreases from 82.24% down to 81.47%, 81.04%, 80.81% and 80.69%. The amount of energy saving is 733 kW, 1,141 kW, 1,365 kW and 1,476 kW which is equivalent to the energy reduction by 0.94%, 1.46%, 1.75% and 1.89%, respectively. If the furnace efficiency is the defined by the ratio between the available heat to the slab and the input heat from the fuel combustion, the furnace efficiency will increase from 69.88% to 70.54%, 70.92%, 71.13% and 71.22%, respectively. However, since the initial cost will increase as the chamber size gets larger. Therefore, the optimization between the energy efficiency improvement and the initial cost of the chamber should be further investigated.

6. Conclusions

The aim of this research is to perform the energy analysis to the preheating chamber and to investigate the effect of the chamber size on the energy efficiency of the 275-tonne/hr reheating furnace. The heat-balance model of the reheating chamber is formulated and applied to the four different chamber sizes, i.e., the capacities of 9, 18, 27 and 36 pieces of slab per one batch. The flue gas temperature and the slab temperatures before and after the waiting period are determined. The result indicates that the average slab temperatures increase to 66.33ºC, 95.57ºC, 119.45ºC and 139.19ºC and decrease down to decrease to 59.52ºC, 75.98ºC, 84.98ºC and 89.46ºC, respectively, after the waiting period. On the other hand, the lowest flue gas temperatures for these four cases are 366.80ºC, 327.37ºC, 296.58ºC and 267.03ºC, respectively, which are all above the predicted acid dew point. The thermal energy carried by the slabs of the consideration cases is 732.9 kW, 1,141.4 kW, 1,364.9 kW and 1,476.1 kW, respectively. By comparing the Sankey diagram before and after the implementation of the reheating chamber, the fuel energy consumption of the consideration cases is reduced by 0.94%, 1.46%, 1.75% and 1.89%. As a result, the furnace efficiency increases from 69.88% to 70.54%, 70.92%, 71.13% and 71.22%, respectively.

References

[1] M. Katsuki and T. Hasegawa, "The science and technology of combustion in highly preheated air," *Symposium (International) on Combustion*, vol. 27, no. 2, pp. 3135–3146, 1998.
[2] T. Hasegawa, S. Mochida, and A. K. Gupta, "Development of advanced industrial furnace using highly preheated combustion air," *Journal of Propulsion and Power*, vol. 18, no. 2, pp. 233-239, 2002.
[3] Q. Jiang, C. Zhang, and J. Jiang, "An industrial reheating furnace with flue gas recirculation modeled by linear transfer functions," *Combustion Science and Technology*, vol. 176, no. 9, pp. 1437-1464, 2004.
[4] W. H. Chen, Y. C. Chung, J. L. Liu, "Analysis on energy consumption and performance of reheating furnaces in a hot strip mill," *International Communications in Heat and Mass Transfer*, vol. 32, No. 5, pp. 695-706, 2005.
[5] M. Si, S. Thompson, and K. Calder, "Energy efficiency assessment by process heating assessment and survey tool (PHAST) and easibility analysis of waste heat recovery in the reheat furnace at steel company," *Renewable and Sustainable Energy Review*, vol. 15, no. 6, pp. 2904-2908, 2011.
[6] M. Shamanian and A. Najafizadeh, "Hot charge of continuously cast slabs in reheating furnaces," *International Journal of ISSI*, vol. 1, no. 1, pp. 35-37, 2004.
[7] M. Ross, "Industrial energy conservation and the steel industry of the United States," *Energy*, vol. 12, no. 10/11, pp. 1135-1152, 1987.
[8] R. G. C. Beerkens and H. P. H. Muijsenberg, "Comparative study on energy-saving technologies for glass furnaces," *Glastechnische Berichte*, vol. 65, no. 8, pp. 216-224, 1992.
[9] S. Charoen, "A study of energy saving for a reheating furnace by reduction of air leak," M.S. thesis, Mechanical Engineering Dept., Chulalongkorn University, Bangkok, Thailand, 2008.
[10] M. J. Moran and H. N. Shapiro, "Reacting mixtures and combustion," in *Fundamentals of Engineering Thermodynamics*, 5th ed. USA: John Wiley & Sons, 2004, ch. 13, pp. 661.
[11] M. Schmidt, "The Sankey diagram in energy and material flow management," *Journal of Industrial Ecology*, vol. 12, no. 1, pp. 82–94, 2008.
[12] A. Martensson, "Energy efficiency improvement by measurement and control: A case study of reheating furnaces in the steel industry," in *Proceedings from the 14th National Industrial Energy Technology Conference*, Houston, TX, April 22-23, 1992, pp. 236-243.
[13] W. Trinks, M. H. Mawhinney, R. A. Shannon, R. J. Reed, and J. R. Carvey, "Industrial heating processes," in *Industrial Furnaces*, 6th ed. New York: John Wiley & Sons, 2004, Ch.1, pp. 7-8.
[14] F. P. Incropera and D. P. Dewitt, "Internal flow," in *Introduction to Heat Transfer*, 5th ed. Singapore: John Wiley & Sons (Asia) Pte Ltd., 2007, ch. 8, pp. 388-390, 485.
[15] F. M. White, "Viscous flow in ducts," in *Fluid Mechanics*, 6th Edition, McGraw-Hill, 2006, Ch.6, pp. 360.
[16] E. H. Verhoff and J. T. Banchero, "Predicting dew points of flue gases," *Chemical Engineering Progress*, vol. 70, no. 8, pp. 71-72, 1974.
[17] Y. H. Kiang, "Predicting dew points of acid gases," *Chemical Engineering*, vol. 88, no. 3, pp. 127, 1981.
[18] A. G. Okkes, "Get acid dew point of flue gas," *Hydrocarbon Processing*, vol. 66, no. 7, pp. 53-55, 1987.

[19] B. ZareNezhad and A. Almanian, "Accurate prediction of the dew point of acidic combustion gases by using an artificial neural network model," *Energy Conversion and Management*, vol. 52, no. 2, pp. 911-916, 2011.

[20] R. K. Srivastavaa, C. A. Millera, C. Ericksonb, and R. Jambhekarb, "Emissions of sulfur trioxide from coal-fired power plants," *Journal of the Air and Waste Management Association*, vol. 54, no. 6, pp. 750-762, 2004.

[21] Y. Tan, E. Croiset, M. A. Douglas, and K. V. Thambimuthu, "Combustion characteristics of coal in a mixture of oxygen and recycled flue gas," *Fuel*, vol. 85, no. 4, pp. 507-512, 2006.